Observation of peritectic couple growth for a hyper-peritectic alloy under microgravity conditions

To cite this article: A Ludwig and J P Mogeritsch 2023 *IOP Conf. Ser.: Mater. Sci. Eng.* **1274** 012032

Observation of peritectic couple growth for a hyper-peritectic alloy under microgravity conditions

A Ludwig, J P Mogeritsch

Department Metallurgy, Montanuniversitaet Leoben, Leoben, Austria

email: johann.mogeritsch@unileoben.ac.at

Abstract: Under specific conditions, peritectic alloys can form microstructures that behave similar to regular eutectic alloys, with two solid phases growing in a coupled manner directly from the melt. This so-called peritectic couple growth (PCG) is significantly affected by convection. Thus, Bridgman-type experiments were performed onboard the International Space Station using the transparent peritectic alloy, tris(hydroxymethyl)aminomethane–neopentyl glycol (TRIS–NPG). Under these purely diffusive conditions, the formation of PCG, its development over time, and its dependence on the applied process conditions were studied. In this paper, we provide novel insights into the appearance of PCG and the challenges associated with corresponding experiments.

1. Introduction

Peritectic reactions are characterised by the transformation of a solid pro-peritectic α-phase and a liquid phase into a new solid peritectic β-phase upon cooling. At the peritectic temperature T_p, the three phases exist in equilibrium with each other. Trivedi [1,2] reported that for an initial composition within the peritectic plateau and for conditions wherein solidification morphologies of both phases are planar and solute transport is only diffusive, two different peritectic layered structures occur. The first structure represents an oscillation of the solute concentration in the liquid ahead of the solid/liquid (s/l) interface, leading to the formation of an alternating nucleation and a growth sequence such that subsequent bands of both the phases are formed parallel to the solidification front [3], and the second structure represents simultaneous and coupled growth of both phases similar to a regular eutectic growth front, called peritectic coupled growth (PCG), which occurs slightly below T_p. Peritectic layered structures have been reported to be extremely sensitive to convection ahead of the solidification front [4]. Consequently, in directional solidification experiments, peritectic alloys exhibit a variety of complex microstructures, such as isothermal PCG, cellular PCG, island bands, and oscillatory tree-like structures [3-5].

Over the past few years, the authors of this study have employed the organic peritectic metal-like solidifying tris(hydroxymethyl)aminomethane–neopentyl glycol (TRIS–NPG) system [6] to investigate the dynamics of the formation of peritectic layered structures [7-10]. The advantage of such a transparent model alloy is that it enables in-situ observations of the occurring phenomena. However, it has also been demonstrated that on Earth, natural convection affects the formation of peritectic layered structures, thereby complicating unambiguous interpretations of observations. Therefore, experiments under purely diffusive conditions were performed aboard the International Space Station (ISS). In this paper, the first observations are presented and discussed.

2. Experimental Set-up and Method

Investigations were performed using alloys of the following organic compounds: TRIS and NPG as model systems for metal-like peritectic solidification. The experiments were conducted between 17 March and 24 April 2021 aboard the ISS using the Bridgman technique. For this purpose, the so-called Transparent Alloy (TA) instrument, specifically designed by the European Space Agency (ESA) for

investigations with organic model substances, was installed in the Microgravity Science Glovebox (MSG) onboard the ISS.

TRIS and NPG are organic substances that exhibit faceted phases at low temperatures and transparent plastic crystals at high temperatures. The plastic TRIS-rich pro-peritectic α-phase forms a body-centred cubic lattice, and the plastic NPG-rich peritectic β-phase forms a face-centred cubic lattice. Barrio et al. [6] investigated the TRIS–NPG phase diagram. Figure 1 presents the peritectic plateau and alloy composition used in the present study. The compounds were supplied as powders by Sigma-Aldrich [12], with a reported purity of 99.9+% for TRIS and 99% for NPG. Both these compounds are extremely hygroscopic [13], which is why all manipulations with organic compounds were performed under a protective atmosphere. The water content of the organic substance NPG was further reduced by drying at 375 K for 24 h. TRIS was used without further processing because it is sensitive to long-term annealing at elevated temperatures. Alloying and filling of special syringes were performed by the authors. The material was then shipped to QinetiQ Space (Antwerp, Belgium) [14], where the cartridges for space experiments (TAC) were filled. The cartridges possessed a solidification volume of 100 mm (length) × 6 mm (width) × 1 mm (depth). Owing to specific requirements for the contact area between the cartridge and hot and cold clamps, only an effective solidification length of 66 mm was available. This length was conceptually separated into six segments, with lengths of 11 mm each. The solidification experiments were conducted only with 'fresh' segments that were never melted before.

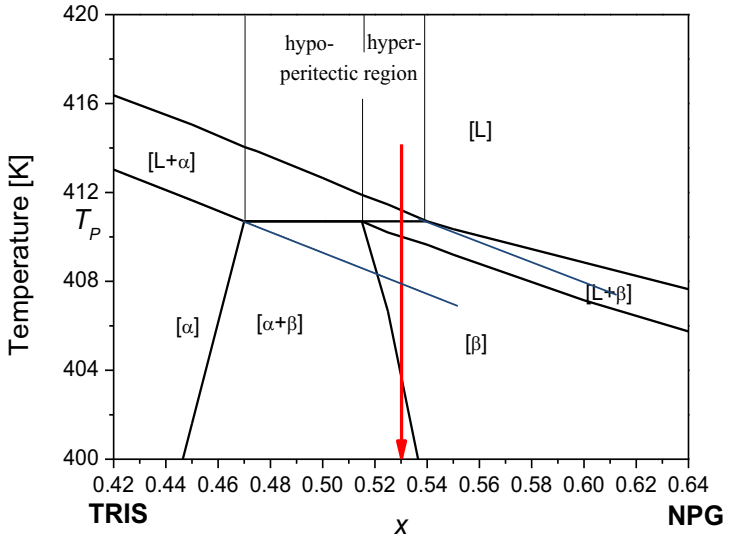

Figure 1. Peritectic region of the TRIS–NPG system. The dashed blue lines represent the metastable extension of the liquidus and solidus lines for the pro-peritectic α-phase. The red arrow indicates the nominal sample composition, x = 0.53 mol fraction of NPG. The peritectic temperature, T_p, is 410.7 ± 0.5 K.

The TA instrument was developed by QinetiQ Space on behalf of the ESA. It was specifically designed for experiments with organic transparent alloys under microgravity (μg) conditions. The instrument is a Bridgman furnace with a control unit and an optical assembly. The furnace consisted of two parallel clamps as a hot zone (rear and front clamp) and two parallel clamps as a cold zone (rear and front clamp), and these zones were separated by an adiabatic zone of 7 mm. This represents the area for optical observation. In the adiabatic zone, a temperature gradient governed by the temperature of the clamps was established.

The optical recording system of the TA apparatus included a light-emitting diode source for illumination and a charge-coupled device camera centred at the adiabatic zone with a field of view (FOV) of 6.1 x 5.1 mm^2. During the experiments, a set of three images was acquired with a time step of 3 s at the following three different focus points: ff_1 = 0 mm, directly on the inside of the front glass wall; ff_2

= 0.5 mm, at the centre of the cartridge; and ff_3 = 0.8 mm, near the rear glass wall. A set of new images was acquired every 30 s. However, only once per hour a set of three images with different focus points was broadcast directly to Earth. The present findings are primarily based on these images.

The experiment we report here will be referred to as TAC4S2. The experiment was performed between 19 April 2021 07:32 GMT and 20 April 2021 06:33 GMT. The nominal alloy composition was 0.53 mol fraction of NPG. The experiment consisted of the following steps. First, the temperature of all clamps was set to 403 K, and the sample was annealed for 2 h. Subsequently, the temperature in the cold zone was set to 379 K, and the temperature in the hot zone was set to 439 K. The sample was maintained at rest for an additional 1 h to achieve thermal equilibrium within the device. For the selected clamp temperatures, we expected a temperature gradient within the adiabatic zone of 3.0 ± 1 K/mm. Thereafter, the cartridge was moved with a constant pulling velocity of V_p = 0.10 µm/s from the hot zone towards the cold zone. Under these conditions, the s/l interface was well-observable within the adiabatic gap. After 22 h of growth, the motion was stopped, and the sample was maintained at rest for another 4 h. The microgravity level during the processing time of TAC4S2 was measured using the 'es09'-sensor at the ceiling right side of the MSG. The mean µgRMS[1] was approximately 2.3 µg between 08:00 and 22:00 GMT and less than 0.5 µg during night's rest for the astronauts[2]. The median frequency measured by the sensor was constant at approximately 0.182 Hz.

3. Results

Immediately after activation of the gradient, liquid appeared at the FOV's 'hot' side. The solid in direct contact with the liquid consisted of several small grains, which immediately began to coarsen and elongate with time. However, as the two involved solid phases are optically indistinguishable, determining whether these grains consisted of the pro-peritectic α- or peritectic β-phase or both was difficult. In addition, several small bubbles were observed. These bubbles formed a substructure in the colder part of the solid, which gradually disappeared at higher temperatures. During pulling, this bubble substructure moved without any visible alteration towards the FOV's 'cold' side until it finally disappeared. Occasionally, larger bubbles were observed in the solid/mush close to the melt.

A few smaller bubbles and tracers in the liquid were tracked during the course of the experiment. The origin of the tracers was unclear. They could be contaminants already present in the purchased components. However, they were extremely small and difficult to observe. The bubbles and tracers tracked with a focus point ff_2 = 0.5 mm were located in the middle of the sample and thus did not stick to the glass walls. Based on the trajectory of the small bubbles, it was confirmed that the solid moved at the pulling speed. The tracers in the liquid, however, moved faster by approximately 4%, indicating the density difference between the solid and liquid phases and, thus, the need for a feeding flow to compensate for solidification shrinkage.

The growth dynamics of the s/l interface morphology are illustrated in figure 2. Note that the images were captured with a focus point at ff_2 = 0.5 mm. Hence, all structures with a sharp appearance are located around the middle of the sample, whereas all blurry patterns appear either in the back or towards the front glass wall. The bright blurry structures lie in the back, and the grey blurry structures appear at the front. Therefore, the image presented is not a top view of the inclined s/l interface as it might seem but a view from beneath. As outlined in another paper written by the authors [10], this inclination of approximately 6–7° against the sample normal was caused by an unplanned thermal bias between the rear and front clamps. In retrospect, this turned out to be useful because the details at the s/l interface were easier to observe through this inclined view.

After 3 h of pulling, solidification occurred with a planar growth of larger grains, which most probably consisted of a single solid phase, that is, either α or β (figure 2a). After 4 h, the growth morphology clearly changed (figure 2b). Patches of a second solid phase could now be identified. Several irregularly surrounded and unconnected patches growing in wavy troughs on the first growing primary solid phase can be observed in figure 2b. After 1 h (figure 2c), the number of patches increased, but their size decreased. In addition, the patches appeared more spherical in shape. After another hour, most of the patches became elongated, and some demonstrated curved shapes (figure 2d). For the next couple of hours, this was the dominant growth morphology, whereby some of the curved lamellae resembled the zigzag lamellae that formed during eutectic growth (figures 2d and e). Furthermore, as

[1] RMS: root-mean-square acceleration
[2] Information taken from „https://gipoc.grc.nasa.gov/pims/roadmap/"

the experiment progressed, the lamellae changed into fibres (figure 2f). It is worth mentioning that as shown in figures 2a–f, the phase that had formed always grew in depressions of the primary phase, independent of its morphology. Only the tip of the growing fibres (cell-like growth, figure 2f) was at the same level (or even higher) as the primary phase. During the entire 22 h of growth, the s/l interface recoiled by approximately 3 mm, which corresponds to an interface temperature reduction of approximately 9 K (assuming a gradient of $G = 3$ K/mm).

After a period of constant pulling, the motion stopped, but the thermal gradient was maintained. Lateral growth of the phase that formed the fibres could now be observed (figure 2g). The fibres turned into patches that increased in size by growing along the s/l interface (figure 2h). Simultaneously, it appeared that the opposite occurred in the background. However, this observation requires more attention and will be considered in detail in the future. Along with the overgrowth, the s/l interface moved toward higher temperatures so that the interface gradually reached a final position at a somewhat higher temperature level.

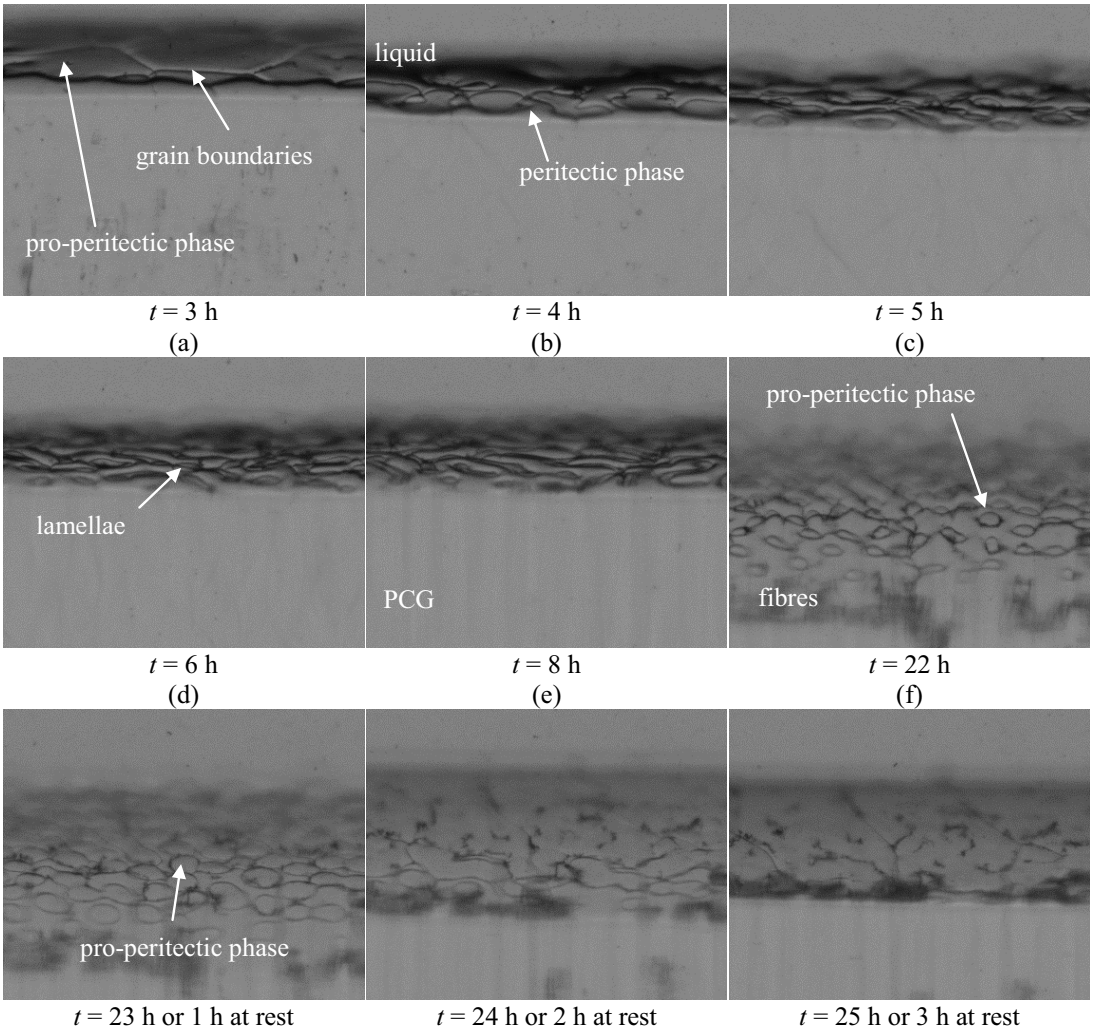

Figure 2. Development of the solidification morphology for a hyper-peritectic alloy with 0.53 mol fraction of NPG at a pulling rate of $V_p = 0.10$ μm/s. The time after which pulling was initiated is indicated below each image. All images have a width of 1 mm.

4. Discussion

Figures 2b–f present the changes occurring in PCG over a duration of more than 18 h. However, the observed phases cannot be clearly classified into α or β phases. Particularly, the occurrence of patches

of the second solid phase after approximately 4 h of growth raised doubts regarding their formation mechanism. Thankfully, in the meantime we have got excess to the full picture set, with pictures being taken every 30 s. It turned out that the patches were formed by unstable finger-like overgrowth of the primary s/l interface with a second solid phase. Nucleation was not involved in this transition. Therefore, it was clear that the patches, which later turned into lamellae and fibres, consisted of the primary solid phase, and the matrix consisted of the second solid phase.

Based on this finding, we determined the identities of the different phases. According to the TRIS–NPG phase diagram (figure 1), solidification should begin with the pro-peritectic α-phase. Thus, it is natural to assume that the primary solid phase, as well as patches, lamellae, and fibres, consisted of the α-phase, and the matrix phase consisted of the β-phase. We have labelled figure 2 accordingly. As the interface continued to recoil to lower temperatures, the amount of the α-phase decreased; hence, the patches transformed into lamellae and later into fibres. This is in consistence with the phase diagram. However, that the α-phase fibres finally cover, at least partly, the s/l interface at the at the end of the experiment is still curious.

With the suggested phase identification in mind, we can now discuss the solidification experiment from the beginning. Clearly, the α-grains grew with a planar but tilted s/l interface (figure 2a). However, the corresponding solutal recoil was far from being completed, as the interface displacement still varied approximately linearly with time. Three hours after the pulling was initiated, the s/l interface moved by 0.4 mm, which corresponds to a reduction of the interface temperature of around 1.2 K. Based on the phase diagram information, this fact leads to an interface temperature of approximately 0.2 K below the peritectic temperature, T_p. Four hours after the initiation of pulling (figure 2b), when the peritectic β-phase first appeared, the interface temperature was approximately 0.5 K below T_p. However, herein, we assumed that the s/l interface temperature after the 1-h thermal gradient stage was just at the liquidus of the nominal alloy composition (1.0 K above T_p). Note that this interface temperature can be lower owing to solutal balancing in solid and liquid phases prior to pulling or due to the squeezing of intergranular segregated liquid from the mush, as recently reported by the authors [10]. More importantly, than the actual temperature at which the β-phase first appeared is the fact that the interface continued to move towards lower temperatures. This indicates that the growth temperature for the subsequent PCG is definitely below T_p.

Figure 2b indicates that the pro-peritectic α-phase patches are located at the interface depressions of the peritectic β-phase. From figures 2b–e, it appears that the pro-peritectic α-phase is unwilling to leave the field for the peritectic β-phase, although the overall interface position continues to move towards lower temperatures. The temperature at the triple line (α-phase, β-phase, liquid) is always at a reduced level, which is understandable from the viewpoint of energy. However, from figures 2b–e, it appears that the mean temperature of the peritectic β-phase is slightly higher than the mean temperature of the pro-peritectic α-phase, and it increases with time. Figures 2b–f also indicate that the typical size of the pro-peritectic α-phase lamellae decreases, until a transition from lamellar growth to fibre growth occurs, attended by a gradual decrease in the interface temperature by approximately 9 K. Evidently, we can conclude that PCG led to an increase in solute accumulation ahead of the front, similar to the initial transient for single-phase growth. It also appears that the amount of α-phase decreased. However, this is not easy to determine quantitatively from the available images. We also observed that the coupled-growth pattern experienced a global drift along the inclined isotherm from the front towards the back. This was also observed in recent studies on growing eutectics with tilted s/l interfaces [15].

5. Conclusions and Summary

The experimental findings based on directional solidification under purely diffusive conditions with a rather small pulling velocity using a hyper-peritectic TRIS–NPG alloy can be summarised as follows:

- Solidification commenced via a planar growth of the pro-peritectic α-phase.
- Below the peritectic temperature, the peritectic β-phase grew over the α/l interface in an unstable manner, such that patches of the pro-peritectic α-phase remained in contact with the liquid.
- These α-phase patches grew simultaneously with the β-phase in a coupled manner, so that PCG established. This growth mode continued for hours, whereby the appearance of the pro-peritectic α-phase changed from patch-like to lamellar and finally to rod-like.

- During growth, the global s/l interface recoiled by approximately 3 mm, which corresponds to a reduction in the interface temperature by approximately 9 K. However, during the 22 h of growth, no steady state was reached. This was evident not only based on the changes in the α-phase growth morphology but also based on the fact that the growth velocity was still lower than the pulling speed.
- After pulling was stopped, the α-phase fibres spread over the s/l interface, at least in some areas. In other areas, the β-phase grew over the α-phase fibres. However, a comprehensive interpretation of these observations is still underway.

Acknowledgements

We thank ESA and QinetiQ Space for aiding in the development of the TA instrument and E-USOC at the Polytechnical University Madrid for their support in performing experiments on the ISS. This research was completed owing to the support provided by ESA for the framework of the project METCOMP and the Austrian Research Promotion Agency (FFG) under grant number 865969.

References

[1] Trivedi R 1995 Theory of layered structure formation in peritectic systems *Metall. Mater. Trans.* **26A** pp 583-90.
[2] Trivedi R 2005 The role of heterogeneous nucleation on microstructure evolution in peritectic systems *Scripta Mater.* **53** pp 47-52.
[3] Boettinger W J 1974 The structure of directionally solidified two-phase Sn-Cd peritectic alloys *Metall.Trans.* **5** pp 2023-2031.
[4] Dobler S, Lo T S , Plapp M, Karma A, Kurz W 2004 Peritectic coupled growth *Acta Mater.* **52**, pp. 2795–2808.
[5] Park J S, Trivedi R 1998 Convection-induced novel oscillating microstructure formation in peritectic systems **187** *J. Cryst. Growth* pp 511-515.
[6] Barrio M, Lopez D O, Tamarit J L, Negrier P, Haget Y 1995 Degree of Miscibility between Non -isomorphous Plastic Phases: Binary System NPG (Neopentyl-glycol)-TRIS [tris(hydroxymethyl)aminomethane] *J. Mater Chem.* **5 (3)** pp 431-439.
[7] Ludwig A, Mogeritsch J P, Grasser M 2009 In situ observation of unsteady peritectic growth modes *Trans. Indian Inst. Met.* **62** pp 433-436.
[8] Mogeritsch J P, Eck S, Grasser M, Ludwig A 2010 In Situ Observation of Solidification in an Organic Peritectic Alloy System *Mater. Sci. Forum* **649** pp 159-164.
[9] Ludwig A, Mogeritsch J P 2011 In situ observation of coupled peritectic growth *John Hunt International Symposium London* pp 233-242.
[10] Ludwig A, Mogeritsch J P, Rettenmayr M 2022 On/off directional solidification of near peritectic TRIS-NPG with a planar but tilted solid/liquid interface under microgravity conditions *Scripta Mater.* **214** p. 114683.
[11] Mogeritsch J P, Sillekens W, Ludwig A 2022 In-situ Observation of Coupled Growth Morphologies in Organic Peritectics under Pure Diffusion Conditions, *TMS annual meeting, Anaheim, California*, ISBN: 978-3-030-92381-5
[12] http://www.sigmaaldrich.com
[13] NPG CAS-No 126-30-7 and TRIS CAS-No 77-86-1.
[14] https://www.qinetiq.com/en/sectors/space
[15] Bottin-Rousseau S, Witusiewicz V T, Hecht U, Fernandez J, Laveron-Simavilla A, Akamatsu S 2022 Coexistence of rod-like and lamellar eutectic growth patterns *Scripta. Mater.* **207** p. 114314